Tellus (2001), 53B, 673–694
Printed in UK. All rights reserved

TELLUS
ISSN 0280–6509

Analysis of regional budgets of sulfur species modeled for the COSAM exercise

By G. J. ROELOFS[1]*, P. KASIBHATLA[2], L. BARRIE[3‡], D. BERGMANN[4], C. BRIDGEMAN[5], M. CHIN[6], J. CHRISTENSEN[7], R. EASTER[8], J. FEICHTER[9], A. JEUKEN[10], E. KJELLSTRÖM[11], D. KOCH[12], C. LAND[9], U. LOHMANN[13] and P. RASCH[14], [1]*Institute for Marine and Atmospheric Research Utrecht (IMAU), Utrecht University, Utrecht, The Netherlands;* [2]*Nicholas School of the Environment, Duke University, Durham, NC, USA;* [3]*Pacific Northwest National Laboratory, Richland, WA, USA;* [4]*Atmospheric Science Division, Lawrence Livermore National Lab, CA, USA;* [5]*Department of Chemistry, University of Cambridge, UK;* [6]*NASA Goddard Space Flight Center, Greenbelt, MD, USA;* [7]*National Environmental Research Institute, Roskilde, Denmark;* [8]*Pacific Northwest National Laboratory, Richland, WA, USA;* [9]*Max Planck Institute for Meteorology, Hamburg, Germany;* [10]*Royal Netherlands Meteorological Institute (KNMI), De Bilt, The Netherlands;* [11]*Department of Meteorology, Stockholm University, Sweden;* [12]*NASA/GISS, New York, NY, USA;* [13]*Atmospheric Science Program, Dalhousie University, Halifax, Canada;* [14]*National Center for Atmospheric Research (NCAR), Boulder, CO, USA*

(Manuscript received 12 October 1999; in final form 11 March 2001)

ABSTRACT

The COSAM intercomparison exercise (comparison of large-scale sulfur models) was organized to compare and evaluate the performance of global sulfur cycle models. Eleven models participated, and from these models the simulated surface concentrations, vertical profiles and budget terms were submitted. This study focuses on simulated budget terms for the sources and sinks of SO_2 and sulfate in three polluted regions in the Northern Hemisphere, i.e., eastern North America, Europe, and Southeast Asia. Qualitatively, features of the sulfur cycle are modeled quite consistently between models, such as the relative importance of dry deposition as a removal mechanism for SO_2, the importance of aqueous phase oxidation over gas phase oxidation for SO_2, and the importance of wet over dry deposition for removal of sulfate aerosol. Quantitatively, however, models may show large differences, especially for cloud-related processes, i.e., aqueous phase oxidation of SO_2 and sulfate wet deposition. In some cases a specific behavior can be related to the treatment of oxidants for aqueous phase SO_2 oxidation, or the vertical resolution applied in models. Generally, however, the differences between models appear to be related to simulated cloud (micro-)physics and distributions, whereas differences in vertical transport efficiencies related to convection play an additional rôle. The estimated sulfur column burdens, lifetimes and export budgets vary between models by about a factor of 2 or 3. It can be expected that uncertainties in related effects which are derived from global sulfur model calculations, such as direct and indirect climate forcing estimates by sulfate aerosol, are at least of similar magnitude.

1. Introduction

The anthropogenic aerosol perturbation of the lower troposphere in the Northern Hemisphere may affect climate with a magnitude comparable to that of the greenhouse gases, although with opposite sign (Schimel et al., 1996). In the first place, the increased aerosol load in the atmosphere reflects more short-wave radiation back to space, which is called the 'direct' effect (Charlson et al., 1992; Kiehl and Briegleb, 1993). In the second place, increasing aerosol number concentrations may influence the microphysical development of

* Corresponding author.
e-mail: G. J.Roelofs@phys.uu.nl
‡ Former affiliation: Environment Canada, Toronto, Canada.

a cloud, which is called the 'indirect' effect. For the same cloud liquid water content, a larger aerosol concentration leads to smaller effective cloud droplet radii and a higher cloud albedo. This may lead to a decrease in the precipitation formation efficiency and a longer cloud lifetime (Twomey, 1974; Albrecht, 1989; Jones et al., 1994; Boucher and Lohmann, 1995, Lohmann and Feichter, 1997). The aerosol climate forcing involves mainly aerosols in the sub-micrometer and micrometer size range which have the highest mass scattering efficiencies, and for which sulfate is an important chemical component.

Globally, anthropogenic sulfur sources exceed natural sources by a factor of 3 to 4 (Spiro et al., 1992). Emissions from fossil fuel burning predominate, and about 90% of the anthropogenic sources are located in the northern hemisphere (NH) (Benkovitz et al., 1996). The NH emissions are concentrated in three industrialized areas in North America, West and Central Europe, and Southeast Asia. The atmospheric lifetime of sulfate is of the order of a few days. Compared to the long-lived greenhouse gases, aerosol concentrations are therefore highly variable in space and time. Moreover, sulfur species may be exported from the polluted regions to relatively clean oceanic regions, and even to neighboring continents (Benkovitz and Schwartz, 1997; Chin et al., 1996). Because the background marine air is relatively clean and contains relatively few aerosols, the export of anthropogenic aerosol to marine environments can have a significant impact on cloud optical properties (Radke et al., 1989; Garrett and Hobbs, 1995) and may lead to a significant negative climate forcing.

Three-dimensional chemistry/transport models that simulate the sources, transports, transformations, and sinks of sulfur-containing species are important tools for the study of the global distribution of sulfate. They enable a better understanding and more accurate estimates of the climate effects of sulfate aerosol, whose uncertainties are large (Schimel et al., 1996). An early attempt to simulate the global sulfur cycle is described by Langner and Rodhe (1991). They used the 3D tropospheric model MOGUNTIA (Crutzen and Zimmerman, 1991) which is driven by monthly averaged wind fields and has a horizontal resolution of $10^\circ \times 10^\circ$ and a vertical resolution of 100 hPa. The model applied monthly averaged OH distributions for the gas phase oxidation of SO_2, whereas aqueous phase oxidation in an air parcel was parameterized using specific time scales for cloud encounter, presence inside cloud, and aqueous phase transformation. Since then, global sulfur models have become more complex and detailed. The resolution of present-day global chemistry models is generally around a few degrees, and the boundary layer usually contains a few layers so that mixing with the free troposphere may be represented realistically. For the oxidation of SO_2, monthly averaged distributions of oxidants may be used (Feichter et al., 1996; Kasibhatla et al., 1997), but in an increasing number of models the production of H_2O_2 is calculated prognostically from HO_2 distributions, or the simulation of the sulfur cycle may be directly coupled to oxidant chemistry (Roelofs et al., 1998). The representation of clouds and precipitation is of major importance for species that are subject to aqueous phase transformation and wet deposition. Some models consider monthly cloud and precipitation fields, e.g., from ISCCP (Pham et al., 1995), or use data from GCMs or ECMWF with a time resolution of a few hours (Chin et al., 1996; Benkovitz et al., 1997). In chemistry–general circulation models, the sulfur cycle is sometimes coupled directly to the simulation of cloud characteristics (Lohmann and Feichter, 1997).

In this study, which is a contribution to the COSAM intercomparison exercise (Comparison of large-scale sulfur models), we examine the sulfur budget terms simulated by eleven global sulfur cycle models. The rationale behind COSAM is to evaluate their performance by analyzing the simulated surface concentrations, vertical profiles and global and regional budgets of sulfur species. An overview of COSAM and its main results is presented by L. Barrie, Y. Yi, W. R. Leaitch, U. Lohmann, P. Kasibhatla, G. J. Roelofs, J. Wilson, F. McGovern, C. Benkovitz, M. A. Melieres, K. Law, J. Prospero, M. Kritz, D. Bergmann, C. Bridgemann, M. Chin, J. Christensen, R. Easter, J. Feichter, C. Land, A. Jeuken, E. Kjellström, D. Koch and P. Rasch, 2000. A comparison of large scale atmospheric sulphate aerosol models (COSAM): Overview and highlights, *Tellus*, this issue (further referred to as: Barrie et al., 2001).

The participating models, one hemispheric and

10 global models, are listed in Table 1. Four models are general circulation models (GCMs; GA, GB, GC, GD), six models are global chemical transport models (CTMs; CA, CB, CC, CD, CE, CF) and one model is a hemispheric chemical transport model (HA). Ten models submitted data for the sulfur cycle and the radon/lead simulations, whereas one model (i.e., CD) submitted data for the radon/lead simulation only. A more elaborate description of the models and their parameterizations is given by U. Lohmann, W. R. Leaitch, L. Barrie, K. Law, Y. Yi, D. Bergmann, C. Bridgemann, M. Chin, J. Christensen, R. Easter, J. Feichter, A. Jeuken, E. Kjellström, D. Koch, C. Land, P. Rasch and G. J. Roelofs, 2000. Vertical distributions of sulfur species simulated by large scale atmospheric models in COSAM: Comparison with observations, *Tellus*, this issue (further referred to as: Lohmann et al., 2001).

Here we analyze and compare the simulated budgets for three industrialized regions, i.e., Eastern North America, Europe and Southeast Asia. The object of the budget comparison is threefold. In the first place, we examine the coherence of the simulated budgets between models. In the second place, we want to identify processes

Table 1. *Participating models, model characteristics and references*

Model code	Full name	Investigator	Horizontal resolution	# vertical levels	Meteorology	Reference
GA	GISS	Koch	$4^\circ \times 5^\circ$	9	generated	Koch et al. (1999)
GB	ECHAM4-IMAU	Roelofs	$3.75^\circ \times 3.75^\circ$	19	generated	Roelofs et al. (1998)
GC	CCCma	Lohmann	$3.75^\circ \times 3.75^\circ$	22	generated	Lohmann et al. (1999)
GD	ECHAM4-MPI	Feichter, Land, Kjellström	$2.8^\circ \times 2.8^\circ$	19	nudged to ECMWF	Feichter et al. (1996)
CA	TOMCAT	Bridgeman, Law	$5.6^\circ \times 5.6^\circ$	31	ECMWF	Law et al. (1998)
CB	KNMI-IMAU	Jeuken, Dentener	$3.75^\circ \times 5^\circ$	19	ECMWF	Dentener et al. (1999)
CC	MIRAGE	Easter	$2.8^\circ \times 2.8^\circ$	24	nudged to ECMWF	Ghan et al. (2001)
CD	IMPACT	Bergmann	$2^\circ \times 2.5^\circ$	46	GEOS	Penner et al. (1998)
CE	GOCART	Chin	$2^\circ \times 2.5^\circ$	20	GEOS	Chin et al. (2000)
CF	NCAR	Rasch	$1.8^\circ \times 1.8^\circ$	26	NCEP	Rasch et al. (1997)
HA	DEHM	Christensen	150 km	12	ECMWF	Christensen (1997)

Model code	Advection	Vertical diffusion	large scale clouds	H_2O_2	$OH/O_3/NO_3$
GA	2nd order moments	none	prognostic	prognostic	imported
GB	Semi-Lagrangian	TKE[2]	prognostic	full	full
GC	Semi-Lagrangian	ML[2]	prognostic	imported	imported
GD	Semi-Lagrangian	TKE	prognostic	imported	imported
CA	2nd order moments	ML	diagnostic	imported	imported
CB	Finite differences	ML	diagnostic	full	full
CC	Finite differences	TKE	prognostic	[3]	imported
CD	Semi-Lagrangian	implicit scheme	diagnostic	[4]	[4]
CE	Semi-Lagrangian	TKE from GOES	diagnostic	imported	imported
CF	Semi-Lagrangian	ML	diagnostic	prognostic	imported
HA	Pseudo-spectral advection (hor); finite elements (ver)	ML	prognostic	none	none

[1]TKE: prognostic variable for turbulent kinetic energy.
[2]ML: mixing length approach.
[3]CC simulates daytime oxidant chemistry with prescribed ozone and NO_x.
[4]CD only simulates radon and lead.

whose contributions to the total sulfur budgets are subject to large model-to-model variability. In the third place, we want to compare simulated export budgets of sulfur species from the polluted regions.

Unfortunately, sulfur budget terms, necessary to compare model data with, can not be inferred from existing observations of sulfur concentrations. Surface measurements of SO_2 and sulfate are available but observations at higher altitudes, i.e., the middle and upper troposphere, are scarce. Model studies indicate that sulfur concentrations at higher altitudes may be not or only to a small extent related to surface concentrations (Chin et al., 1996). Additionally, sulfur concentrations are often highly variable on regional scales so that a few observed sulfur concentration profiles are probably not representative for a specific region. Observed wet deposition fluxes for sulfate may provide some information about the horizontal distribution of sulfate but not about separate contributions by transport, oxidation and deposition processes to regional or global sulfur distributions. Therefore, we do not attempt to evaluate the performance of individual models, but we limit this study to identification of common features and discrepancies between models, and use the relative agreement between models as a yardstick for uncertainties associated with components of the sulfur cycle. We note that the accompanying papers by Berrie et al. (2001) and Lohmann et al. (2001) present and discuss comparisons between simulated and observed surface concentrations and vertical profiles for sulfur species, radon and lead.

Obviously, detailed sensitivity studies covering transport processes, gas and aqueous phase chemistry, and dry and wet deposition are required to attribute differences between models directly to specific processes and/or parameterizations. However, as global chemistry models have become more and more complex, this would require an enormous effort of the modelers and imply analysis of huge amounts of data. This is not feasible during a single intercomparison exercise. Instead, in this study and in the papers by Barrie et al. (2001) and Lohmann et al. (2001) models are compared "as they are", so that the results of COSAM reflect the performances of global scale sulfur models in the way they are used in present-day atmospheric chemistry and climate research. We note that sensitivity studies regarding specific processes and parameterizations exist, e.g., for convection (Mahowald et al., 1995) and for dry deposition (Ganzeveld et al., 1998).

Section 2 gives a summary of the task posed to the participants and describes the model statistics used for this analysis. In Section 3 the budget terms for SO_2 and sulfate of ten models are presented and compared. Section 4 focuses on the differences in vertical transport efficiencies between models and the impact on the vertical distributions of Rn, SO_2 and sulfate. In Section 5 the simulated export of pollutants from the industrialized regions is examined. Finally, in Section 6 the results are summarized and discussed.

2. Methodology

To achieve the objectives listed in Section 1, all participants were asked to submit their simulated atmospheric burdens and fluxes of emissions, dry and wet deposition, and gas and aqueous phase oxidation of species from the sulfur cycle (DMS, MSA, SO_2 and sulfate) for 4 regions: Eastern North America (ENA, 25°–60°N and 60°–100°W), European region (EMEP; 40°–60°N, 10°W–40°E), Southeast Asia (SEA; 15°–45°N, 105°–140°E), and Southern Ocean Biogenic Source Region (SOBSR; 0°–60°W, 45°–70°S). In order to be able to analyze transport and deposition processes in more detail, similar data were asked for radon (^{222}Rn), which is considered to have a fixed source at the surface and constant lifetime determined by radioactive decay, and lead (^{210}Pb), which is removed from the atmosphere as aerosol. Liquid water content and precipitation budgets were also requested. Additionally, participants were requested to calculate transport budgets for sulfur into and/or out of the 4 regions, and the partitioning of each budget term between below and above 2.5 km altitude, roughly corresponding to the lower and free troposphere. The budget terms are for the winter (DJF) and the summer (JJA). Finally, annual global budget terms were submitted which are discussed by Barrie et al. (2001).

The amount of data for the budget exercise turned out to be quite large, and there are many ways to represent and analyze the data. To keep this paper within reasonable length the authors decided to focus on the simulation of SO_2 and sulfate in the three polluted NH regions (ENA,

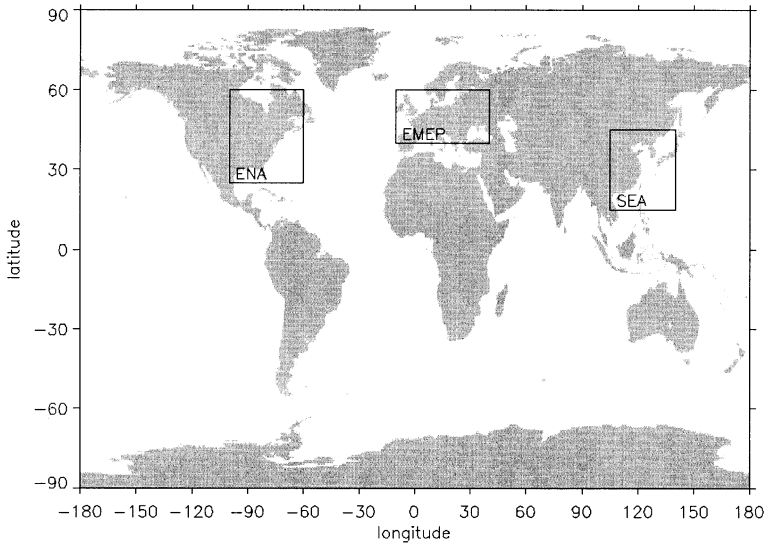

Fig. 1. The three regions for the COSAM sulfur budget intercomparison.

EMEP, SEA shown in Fig. 1). Also, it was decided to analyze regional column-integrated budgets only, although vertical transport efficiencies are examined qualitatively. It was found that submitted export terms did not always match the other budget terms. However, the global budgets (i.e., zero import or export) are closed within 1% for half of the models, and within 2% for all models except one (GD). The few percent difference between sources and sinks may be attributed to year-to-year variabilities in meteorological parameters or, for models with explicit treatment of oxidant formation, the simulated oxidation capacity. We conclude that the simulated budget terms balance, but that the bookkeeping of the fluxes into and out of the region is not always performed correctly. To compare modeled export terms in a consistent way, we inferred these by calculating the residual between the submitted source and sink terms for SO_2 and sulfate. In view of the relatively short lifetimes of SO_2 and sulfate, of the order of a few days, differences between column burdens at the start and the end of the integration periods are insignificant compared to the seasonal budget terms.

3. Regional sulfur budgets

3.1. Regional SO_2 column budgets

Table 2 shows the simulated burden and source, sink and inferred export budgets for SO_2 for the EMEP, ENA, and SEA regions for summer and winter from the models in this intercomparison, except for CD who performed a simulation of Rn and Pb only. For HA, which is not a global model, results are presented for ENA and EMEP only. The budget terms are scaled by the area of each region, so that all results are presented as column budgets. One must be cautious, however, in comparing the column budgets for different regions. The fraction of ocean surface is relatively small in the EMEP region and large in the ENA and SEA regions (Fig. 1). Because sulfur emissions from oceans are relatively small, different ocean fractions lead to artificial differences between area averaged budgets of, for example, SO_2 emissions. Also, the ocean surface fraction influences the relative amount of emitted SO_2 that is transformed to sulfate before it is exported from the region or deposited. The data from Table 2 are averaged in Table 3 with the standard deviation derived from the model-to-model variability, and the relative contribution of individual source/sink terms to the total SO_2 source/sink. In this study we define the relative model uncertainty as the computed standard deviation divided by the average budget term. Because the submitted global budget submitted by GD did not balance properly their results are not used for this table. Note that HA is not considered in the average gas and aqueous phase

Table 2. *Simulated seasonal and regional budgets for SO_2. Column burdens are in mg S m^{-2}; fluxes in mg S m^{-2} day^{-1}*

ENA DJF	CA	CB	CC	CE	CF	GA	GB	GC	GD	HA[1]
emissions	2.40	2.48	2.45	2.47	2.45	2.66	2.40	2.48	2.64	2.42
gas-phase production	0.03	0.10	0.08	0.06	0.05	0.00	0.10	0.12	0.10	0.00
dry deposition	−1.02	−1.47	−1.33	−1.45	−1.17	−1.46	−1.37	−1.41	−1.57	−0.53
wet deposition	−0.12	0.00	−0.05	−0.07	−0.12	−0.12	−0.20	−0.03	−0.04	−0.67
gas-phase oxidation	−0.11	−0.19	−0.03	−0.16	−0.14	−0.18	−0.11	−0.12	−0.09	−0.83
aqueous-phase oxidation	−1.19	−0.50	−0.78	−0.38	−1.00	−0.39	−0.48	−0.98	−0.98	
inferred export	0.01	−0.41	−0.33	−0.46	−0.07	−0.50	−0.33	−0.08	−0.05	−0.39
column burden	2.87	10.62	3.37	5.63	3.96	8.08	5.05	4.24	4.04	3.37
ENA JJA										
emissions	2.19	2.36	2.32	2.29	2.31	2.46	2.23	2.36	2.51	2.25
gas-phase production	0.06	0.06	0.07	0.06	0.06	0.00	0.09	0.15	0.11	0.00
dry deposition	−0.75	−0.57	−0.71	−0.33	−0.58	−0.71	−0.79	−0.83	−1.03	−0.40
wet deposition	−0.14	0.00	−0.26	−0.61	−0.02	−0.05	−0.36	−0.01	−0.06	−0.51
gas-phase oxidation	−0.90	−0.75	−0.17	−0.56	−0.25	−0.65	−0.44	−0.71	−0.92	−1.06
aqueous-phase oxidation	−0.47	−1.03	−1.21	−0.53	−1.35	−1.20	−0.66	−0.50	−0.63	
inferred export	0.01	−0.07	−0.10	−0.32	−0.15	0.15	−0.06	−0.46	0.02	−0.29
column burden	2.79	3.07	1.71	3.04	2.11	2.95	1.54	2.95	3.48	2.33

EMEP DJF	CA	CB	CC	CE	CF	GA	GB	GC	GD	HA
emissions	7.72	7.92	7.74	7.42	7.04	7.95	7.55	7.20	7.94	7.29
gas-phase production	0.02	0.18	0.07	0.07	0.03	0.00	0.17	0.11	0.11	0.00
dry deposition	−3.22	−4.62	−3.70	−4.02	−3.67	−3.84	−3.65	−3.14	−4.64	−1.87
wet deposition	−0.34	0.00	−0.10	−0.01	−0.29	−0.30	−0.18	−0.06	−0.08	−1.35
gas-phase oxidation	−0.11	−0.20	−0.03	−0.14	−0.13	−0.17	−0.11	−0.08	−0.05	−1.66
aqueous-phase oxidation	−2.23	−0.34	−1.86	−0.26	−1.45	−0.60	−0.80	−1.66	−1.56	
inferred export	−1.83	−2.94	−2.13	−3.06	−1.52	−3.05	−3.00	−2.38	−1.72	−2.41
column burden	9.64	18.79	8.39	12.44	7.90	16.49	8.91	10.01	8.18	8.95
EMEP JJA										
emissions	4.65	4.92	4.77	4.46	4.83	4.94	4.63	4.61	4.88	4.40
gas-phase production	0.06	0.11	0.08	0.08	0.06	0.00	0.13	0.18	0.27	0.00
dry deposition	−1.56	−1.64	−1.57	−1.06	−1.68	−1.89	−1.66	−1.31	−2.25	−0.84
wet deposition	−0.55	0.00	−0.30	−0.44	−0.03	−0.04	−0.45	−0.01	−0.06	−1.06
gas-phase oxidation	−1.15	−1.06	−0.29	−1.11	−0.58	−0.96	−0.75	−0.71	−0.96	−1.87
aqueous-phase oxidation	−1.34	−1.61	−2.24	−1.10	−1.91	−1.65	−1.05	−1.56	−1.19	
inferred export	−0.10	−0.72	−0.53	−0.82	−0.69	−0.40	−0.83	−1.18	−0.68	−0.63
column burden	5.18	6.24	3.81	5.38	5.10	5.71	3.56	4.54	5.67	4.45

SEA DJF	CA	CB	CC	CE	CF	GA	GB	GC	GD	HA
emissions	3.13	3.48	3.19	3.15	2.94	3.38	2.80	3.25	3.60	
gas-phase production	0.04	0.06	0.08	0.07	0.06	0.00	0.10	0.11	0.06	
dry deposition	−1.42	−2.31	−1.62	−1.97	−1.39	−2.06	−1.54	−1.62	−2.13	
wet deposition	−0.16	0.00	−0.06	−0.07	−0.04	−0.08	−0.28	−0.03	−0.02	
gas-phase oxidation	−0.38	−0.42	−0.08	−0.38	−0.22	−0.32	−0.29	−0.30	−0.20	
aqueous-phase oxidation	−0.94	−0.80	−1.09	−0.68	−1.26	−0.83	−0.94	−1.59	−1.32	
inferred export	−0.26	−0.01	−0.41	−0.13	−0.10	−0.08	0.14	0.18	0.02	
column burden	5.25	10.87	4.87	7.63	4.64	8.91	6.75	6.11	4.96	
SEA JJA										
emissions	2.48	2.87	2.67	2.52	2.50	2.68	2.26	2.70	2.98	
gas-phase production	0.05	0.06	0.06	0.05	0.05	0.00	0.07	0.12	0.13	
dry deposition	−0.79	−1.02	−0.74	−0.50	−0.69	−0.84	−0.69	−0.70	−1.28	
wet deposition	−0.22	0.00	−0.22	−0.64	−0.02	−0.04	−0.45	−0.03	−0.11	
gas-phase oxidation	−0.83	−0.58	−0.18	−0.47	−0.20	−0.54	−0.44	−0.53	−0.60	
aqueous-phase oxidation	−0.62	−1.21	−1.37	−0.74	−1.48	−1.55	−0.76	−1.15	−1.09	
inferred export	−0.08	−0.11	−0.29	−0.22	−0.16	0.29	0.03	−0.44	−0.04	
column burden	2.68	2.39	1.46	2.10	1.90	3.17	1.53	2.13	2.31	

[1]HA does not distinguish between gas phase and aqueous phase oxidation of SO_2; Table lists total oxidation.

Table 3. *Simulated seasonal and regional budgets for SO_2; column burdens are in mg S m^{-2}; fluxes in mg S m^{-2} day^{-1}; average, standard deviation (σ) and relative contribution*

	DJF			JJA		
	average	σ	%	average	σ	%
ENA						
emissions	2.47	0.08	98	2.31	0.08	97
gas-phase production	0.06	0.04	2	0.06	0.04	3
dry deposition	−1.24	0.31	−49	−0.63	0.17	−26
wet deposition	−0.15	0.20	−6	−0.22	0.23	−9
gas-phase oxidation	−0.13	0.05	−5	−0.55	0.25	−23
aqueous-phase oxidation	−0.71	0.31	−28	−0.87	0.37	−36
total oxidation	*−0.84*	*0.28*		*−1.38*	*0.30*	
inferred export	−0.28	0.19	−11	−0.14	0.19	−6
column burden	5.24	2.56		2.50	0.59	
EMEP						
emissions	7.54	0.32	99	4.69	0.19	98
gas-phase production	0.07	0.07	1	0.08	0.06	2
dry deposition	−3.52	0.76	−47	−1.47	0.33	−30
wet deposition	−0.29	0.42	−4	−0.32	0.35	−7
gas-phase oxidation	−0.12	0.05	−2	−0.83	0.30	−17
aqueous-phase oxidation	−1.15	0.75	−15	−1.56	0.40	−32
total oxidation	*−1.31*	*0.68*		*−2.32*	*0.31*	
inferred export	−2.48	0.57	−33	−0.66	0.30	−14
column burden	11.28	3.87		4.89	0.87	
SEA						
emissions	3.16	0.22	98	2.59	0.18	98
gas-phase production	0.06	0.04	2	0.06	0.03	2
dry deposition	−1.74	0.33	−54	−0.75	0.15	−28
wet deposition	−0.09	0.09	−3	−0.20	0.23	−8
gas-phase oxidation	−0.30	0.11	−9	−0.47	0.21	−18
aqueous-phase oxidation	−1.02	0.29	−31	−1.11	0.36	−42
total oxidation	*−1.31*	*0.27*		*−1.57*	*0.30*	
inferred export	−0.08	0.20	−3	−0.12	0.22	−5
column burden	6.88	2.17		2.17	0.57	

oxidation budgets since it does not separate between these two processes. However, in the total (gas and aqueous phase) oxidation budget in Table 3 HA is included. As a result, the added average gas and aqueous phase oxidation budget does not exactly correspond with the average total oxidation budget.

The principal source of SO_2 in each region is primary emissions. Although the geographical distribution of SO_2 emissions was specified, small differences exist in the reported emissions between models because the actual geographical regions used in the budget analysis differed from model to model due to differences in grid resolutions. The second source of SO_2, i.e., chemical production from DMS oxidation, varies widely between models but is of minor importance in the regional SO_2 budgets considered here. Dry deposition is the dominant sink for SO_2, removing about 50% in winter and 30% in summer. It is simulated consistently between models, with a relative model uncertainty of about 15% or less. Wet deposition of SO_2 appears to be a small term that does not influence the SO_2 budget much. The uncertainty is relatively large, as will be discussed later in this section.

During winter, gas phase oxidation of SO_2 by OH is relatively unimportant, although in SEA, which is located south compared to ENA and EMEP, it removes about 10% of the SO_2. In summer around 20% of the SO_2 is oxidized by OH. Aqueous phase oxidation is an important sink throughout the year, removing up to 42% of the SO_2. In view of the relative importance of

both oxidation processes in the SO_2 budget, it is evident that the relative model uncertainties, which are 35–45% for the gas phase oxidation in summer and between 25 and 65% for the aqueous phase oxidation depending on season and region, can have a large impact on the representation of the sulfur cycle.

The transport of SO_2 into (import, positive) and out of (export, negative) a region affects the regional SO_2 budget. In general, inferred export rates for SO_2 are below 10% of the primary SO_2 emission rates except for the EMEP region. As mentioned earlier, differences between regions may be partly caused by the fraction of ocean surface, which influences the calculated efficiency of chemical transformation relative to the emission budget. Also, oxidation efficiencies are somewhat smaller in EMEP compared to the other, more southerly located, regions so that the transformation to sulfate is slower. Consequently, all models simulate that the net export rate of SO_2 out of the EMEP region is higher in winter than in summer.

Finally, model averaged column SO_2 burdens for the winter more than double those for the summer in all three regions. Largest winter to summer ratios are calculated for SEA. Note that, in contrast, the largest seasonal cycle in primary SO_2 emissions occurs in the EMEP region and not in the SEA region. The SEA region is located relatively close to the summer position of the Intertropical Convergence Zone (ITCZ), an area characterized by strong convective activity which separates the meteorological northern and southern hemispheres, so that a strong seasonality in cloud occurrence may exist.

Despite the underlying similarities, the models display considerable differences in the simulated regional SO_2 burdens. In the Figs. 2, 3 and 4 plots are shown of some important simulated seasonal SO_2 budget terms and first order removal rates for ENA, EMEP and SEA, respectively. The panels a in Figs. 2, 3 and 4 show the simulated seasonal column SO_2 burdens. The simulated burdens differ by as much as a factor of 4 depending on the region and season considered, with CB, CE and GA simulating the largest SO_2 burdens. In summer, when oxidation of SO_2 is more efficient, differences between models are much smaller. There is also a considerable range in the ratio of winter to summer column SO_2 burdens predicted in each region. Predictions of seasonal ratios range from 1 to 3.5 in the ENA region, 1.5 to 3 in the EMEP region, and 2 to 4.5 in the SEA region. The models CB and GB (all regions) and GA (ENA and EMEP) consistently simulate large winter to summer ratios, and CA, CF and GD simulate relatively small ratios.

There exist considerable model-to-model differences in the rates of the individual SO_2 sinks. Panels b, c, d and e in Figs. 2, 3 and 4 show pseudo first-order rate constants for dry deposition, wet deposition, gas-phase oxidation, and aqueous-phase oxidation, respectively, for the three regions. These rate constants, hereafter referred to as 'efficiencies', are defined as the calculated sink term for a process divided by the SO_2 column burden. Note that HA does not separate gas phase and aqueous phase oxidation. As noted earlier, dry deposition (panel b) is the dominant sink for SO_2 in winter. Differences between models generally range over a factor of 2, up to a factor of 4 in ENA in summer. The data suggest that the dry deposition efficiency is somewhat larger in CTMs with a relatively high vertical resolution (CA, CC, CF) than in CTMs with a smaller vertical resolution (CB and CE). On the other hand, the GCMs GB, GC and GD, which have a comparable vertical resolution, simulate highly different deposition efficiencies. Since most models apply the resistance-in-series parameterization for dry deposition, probably the parameterization of the leaf area index (LAI) and soil humidity applied in the models lead to additional differences. There is no clear distinction between models that apply a prognostic variable for turbulent kinetic energy and models that apply a mixing length approach in the calculation of vertical diffusion (Table 1). Direct wet deposition of SO_2 (panel c) is of some importance in CA, CC, CE, GB and HA, but rather insignificant in the other models. This is partly explained by the definition applied in the model. In CC, CE, GB and HA (but also in GC who simulate negligible SO_2 wet deposition) the SO_2 wet deposition budget includes not only SO_2 in precipitation that reaches the surface, but also SO_2 taken up in cloud or rain water that is oxidized before being deposited. The latter contribution is relatively large in summer when oxidant concentrations maximize.

Gas phase oxidation of SO_2 by OH (panel d) is small in winter in all models. On average, the

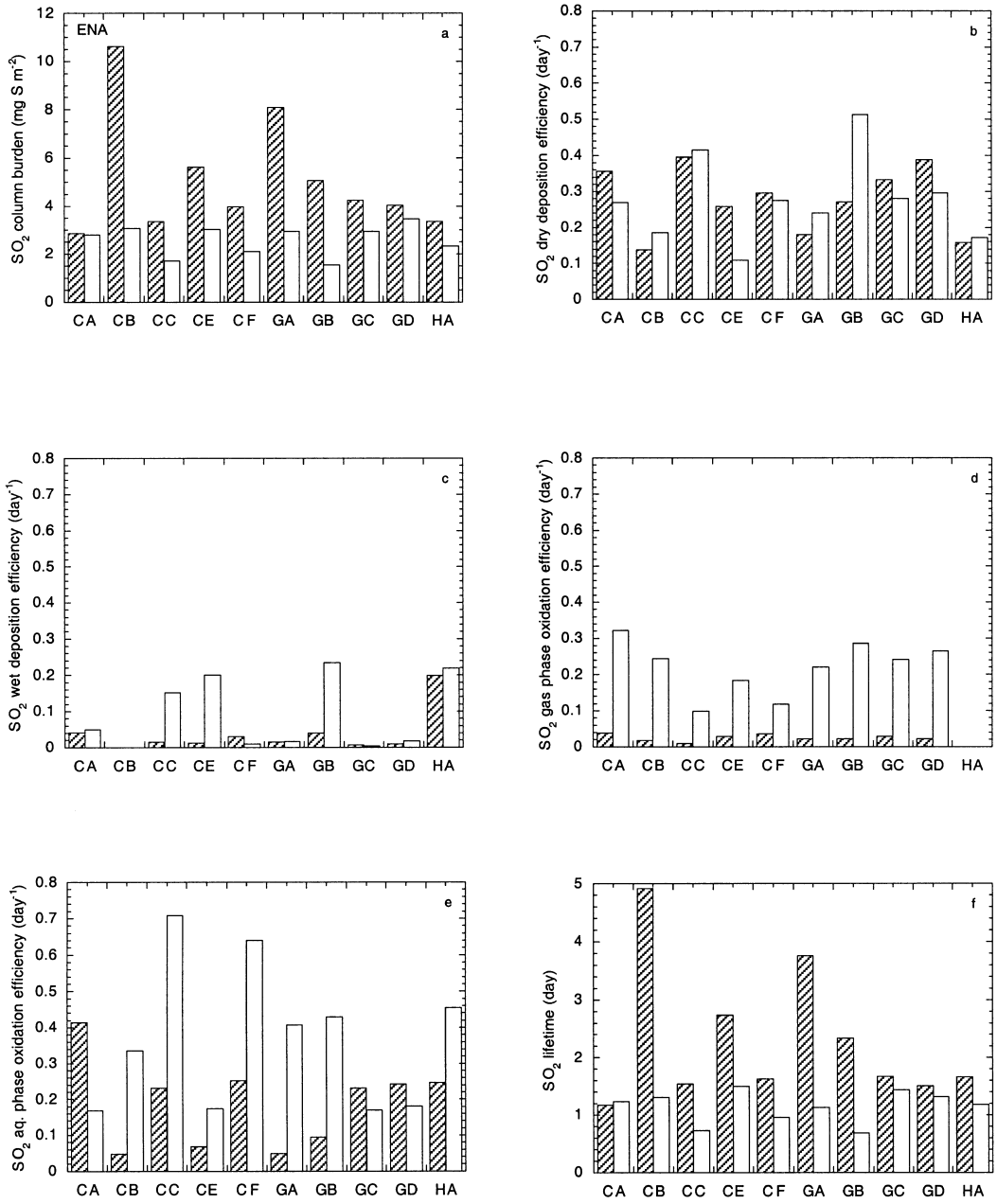

Fig. 2. Simulated SO_2 budget and removal terms for the ENA region. (a) Column burden (mg S m^{-2}), (b) dry deposition efficiency (day^{-1}), (c) wet deposition efficiency (day^{-1}), (d) gas phase oxidation efficiency (day^{-1}), (e) aqueous phase oxidation efficiency (day^{-1}), and (f) lifetime (day). Seasons are DJF (shaded bars) and JJA (white bars).

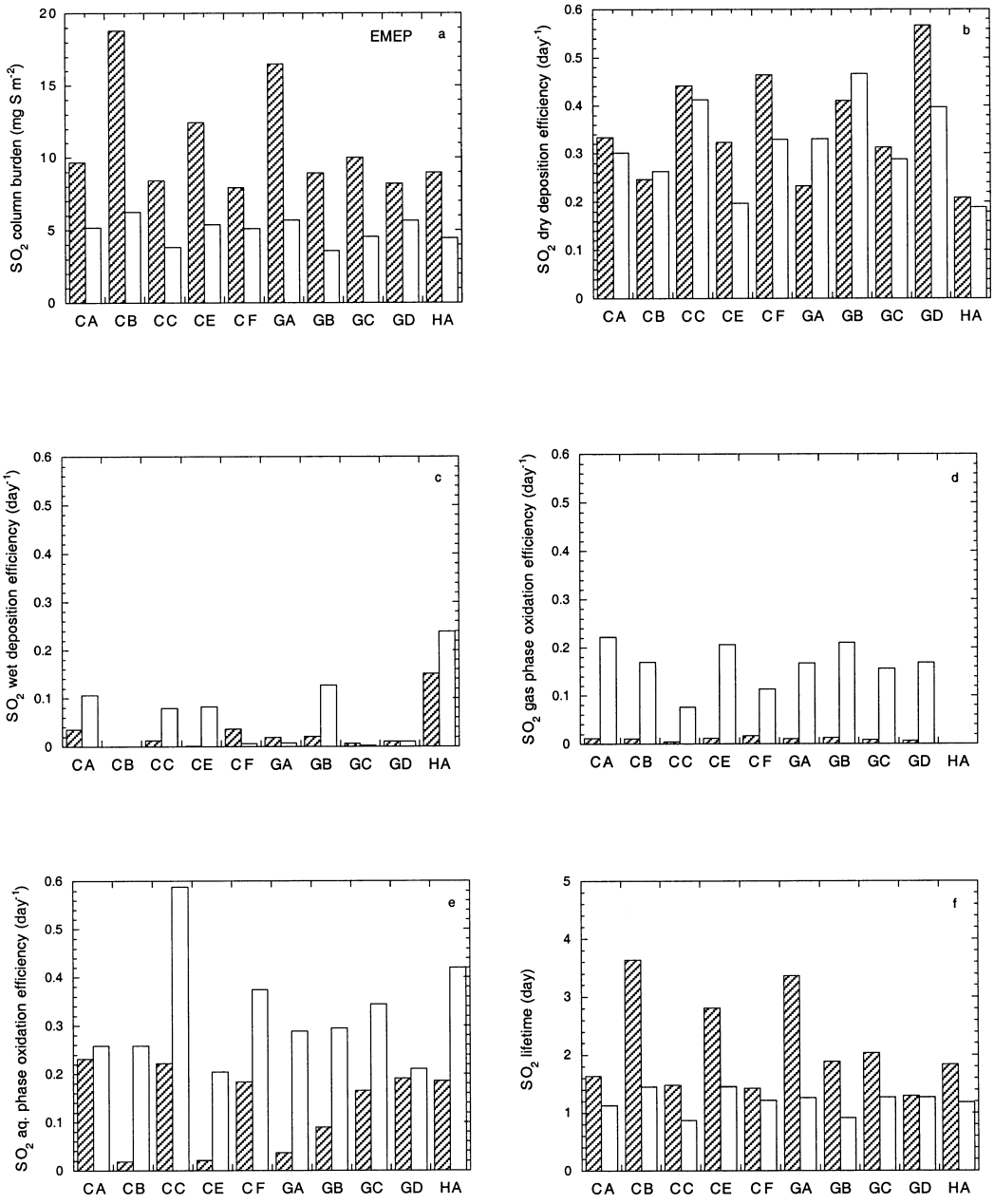

Fig. 3. As Fig. 2 but for the EMEP region.

aqueous phase oxidation efficiency (panel e) is of the same order of magnitude as the dry deposition efficiency. Generally, aqueous phase oxidation of SO_2 is more efficient in summer than in winter due to the larger abundance of oxidants. In summer, aqueous oxidation efficiencies vary up to a factor of 5 between models, but in terms of sulfate production these differences are compensated somewhat by differences in the simulated gas phase oxidation efficiencies, which maximize in

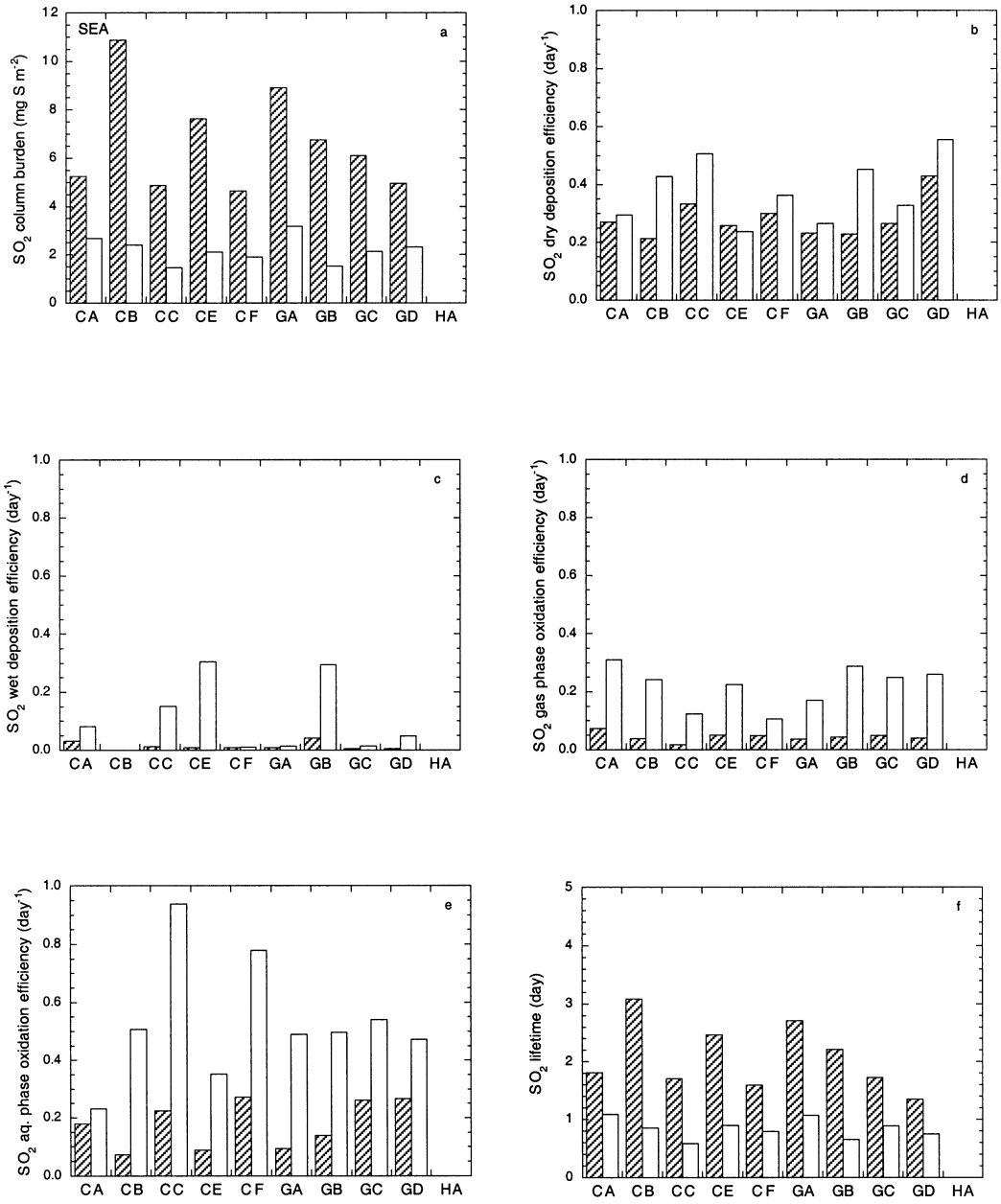

Fig. 4. As Fig. 2 but for the SEA region.

summer and vary up to a factor of 2 between models. The relatively low gas phase oxidation efficiency in CC is attributed to underprediction of OH in the boundary layer, where most SO_2 resides.

In winter, the models separate into two groups characterized by relatively high (CA, CC, CF, GC, GD, HA — note that HA does not separate between oxidation in the gas phase and the aqueous phase) and low aqueous phase oxidation rates

(CB, CE, GA, GB). This seems related to whether full chemistry is applied in the models (i.e., the simulation of the oxidant concentrations and the sulfur cycle is coupled), or monthly averaged ozone and hydrogen-peroxide distributions are imported (Table 1). Models that apply a full chemistry or prognostic approach are expected to yield lower sulfate rates from oxidation by H_2O_2 especially in winter when they represent oxidant limited conditions more realistically (Roelofs et al., 1998). The relation appears to be valid for GC and GD, who import monthly averaged oxidant fields and simulate relatively high oxidation rates in winter, and for CB, GA and GB, who calculate oxidant fields interactively or prognostically and simulate relatively small oxidation efficiencies in winter, but not for CA, CC and CE. Note that Lohmann et al. (2001) also find a difference between both approaches: they conclude that models with full oxidant chemistry tend to agree better with observations. Additionally, the data suggest that the SO_2 aqueous phase oxidation efficiency in winter is somewhat larger in CTMs with a relatively high vertical resolution (CA, CC, CF) than in CTMs with a smaller vertical resolution (CB and CE).

The model-to-model differences in the column SO_2 burdens described earlier are the result of the significant differences in the SO_2 sink terms and lifetimes, the latter of which are shown in panels f in Figs. 2, 3 and 4. The SO_2 lifetimes are defined as the column SO_2 burden divided by the column SO_2 deposition and oxidation budgets. In all models and in all regions (except the CA model in the ENA region) the column SO_2 lifetime is longer in winter than in summer. Note that CB, CE and GA, who simulate relatively large SO_2 burdens and lifetimes in winter, consistently simulate small aqueous oxidation efficiencies in winter. The CTMs with a relatively high vertical resolution (CA, CC, CF) simulate smaller SO_2 lifetimes than the CTMs with a smaller vertical resolution (CB and CE), in accordance with the larger dry deposition and aqueous phase oxidation efficiencies. However, we do not find a distinction between models based on their horizontal resolution.

3.2. *Regional sulfate column budgets*

Table 4 shows the simulated source, sink and inferred export budgets of column sulfate for the EMEP, ENA, and SEA regions for summer and winter, as well as the computed column sulfate. The detailed data from Table 4 are summarized in Table 5, in a similar way as Table 3.

Primary sulfate emissions are mostly of minor importance as a sulfate source, except when other sulfate production pathways are relatively low (as in CB and CE in EMEP in winter). Primary sulfate emissions were not directly specified, and on average the models assume these emissions to range between 4 to 16% of the anthropogenic sulfur emissions depending on the region and the season (Table 5). Generally, aqueous phase oxidation of SO_2 is the dominant sulfate source, contributing on average 73–78% in winter and 59–67% in summer. The relative model uncertainty is between 28% in SEA to 65% in EMEP in winter. Gas-phase SO_2 oxidation is less important in winter as a sulfate source. Wet deposition is the major sulfate removal process in all models, being a few times more effective as dry deposition in each region and season. The relative model uncertainty is rather large, between 20% (SEA, summer) and 50% (EMEP, winter).

There is a near-consensus among models that there is net export of sulfate from each of the three regions, and that the export from the EMEP region is larger than the export from the SEA and the ENA regions. The contribution of export to the total sink is about the same in winter and summer in ENA and EMEP. Due to large differences in the simulated source and deposition terms, the relative model uncertainty for sulfate export is large, from about 50% for SEA in winter to about 90% for EMEP in winter.

In Figs. 5, 6 and 7 plots are shown of some important seasonal sulfate budget terms for ENA, EMEP and SEA, respectively. Panels a in Figs. 5, 6 and 7 show simulated winter and summer column sulfate burdens. Sulfate column burdens range between about 1–6 mg S m^{-2} in winter and 2–8 mg S m^{-2} in summer, depending on region, whereas model-to-model variabilities can be as large as a factor of three in winter. In contrast to the simulated seasonal cycle of column SO_2, simulated sulfate contents are generally larger in summer than in winter (note that CA, CE and GC simulate an opposite seasonality in the SEA region). This seasonality is associated with the SO_2 oxidation efficiencies, which minimize in summer and maximize in winter.

Table 4. *Simulated seasonal and regional budgets for sulfate; column burdens are in mg S m^{-2}; fluxes in mg S m^{-2} day^{-1}*

ENA DJF	CA	CB	CC	CE	CF	GA	GB	GC	GD	HA[1]
emissions	0.05	0.10	0.05	0.04	0.05	0.08	0.12	0.00	0.00	0.13
gas-phase production	0.11	0.19	0.03	0.16	0.14	0.18	0.11	0.12	0.09	0.83
aqueous-phase production	1.19	0.50	0.78	0.38	1.00	0.39	0.48	0.98	0.98	
dry deposition	−0.10	−0.07	−0.16	−0.06	−0.04	−0.12	−0.12	−0.13	−0.10	−0.26
wet deposition	−0.92	−0.56	−0.47	−0.49	−1.15	−0.34	−0.56	−0.56	−0.83	−0.42
inferred export	−0.32	−0.16	−0.22	−0.04	−0.00	−0.19	−0.03	−0.41	−0.15	−0.29
column burden	2.90	2.51	2.62	1.94	1.19	2.18	2.39	3.89	2.23	1.86
ENA JJA										
emissions	0.04	0.10	0.05	0.03	0.05	0.07	0.11	0.00	0.00	0.12
gas-phase production	0.90	0.75	0.17	0.56	0.25	0.65	0.44	0.71	0.92	1.06
aqueous-phase production	0.47	1.03	1.21	0.53	1.35	1.20	0.66	0.50	0.63	
dry deposition	−0.18	−0.10	−0.23	−0.06	−0.09	−0.33	−0.16	−0.12	−0.20	−0.28
wet deposition	−0.84	−1.40	−0.74	−1.05	−1.33	−1.39	−0.87	−1.20	−1.32	−0.43
inferred export	−0.39	−0.38	−0.46	−0.00	−0.23	−0.20	−0.20	0.11	−0.02	−0.49
column burden	4.37	5.74	4.36	2.34	3.30	5.31	5.61	4.34	6.15	2.74

EMEP DJF	CA	CB	CC	CE	CF	GA	GB	GC	GD	HA
emissions	0.16	0.30	0.16	0.39	0.14	0.24	0.39	0.00	0.00	0.38
gas-phase production	0.11	0.20	0.03	0.14	0.13	0.17	0.11	0.08	0.05	1.66
aqueous-phase production	2.23	0.34	1.86	0.26	1.45	0.60	0.80	1.66	1.56	
dry deposition	−0.21	−0.09	−0.27	−0.08	−0.05	−0.18	−0.17	−0.14	−0.11	−0.43
wet deposition	−0.79	−0.51	−1.18	−0.60	−1.59	−0.53	−0.81	−0.44	−1.19	−0.57
inferred export	−1.50	−0.23	−0.60	−0.11	−0.08	−0.29	−0.32	−1.17	−0.31	−1.04
column burden	5.14	2.59	3.44	2.17	1.26	2.88	2.75	5.51	2.51	3.64
EMEP JJA										
emissions	0.10	0.19	0.10	0.23	0.10	0.14	0.24	0.00	0.00	0.23
gas-phase production	1.15	1.06	0.29	1.11	0.58	0.96	0.75	0.71	0.96	1.87
aqueous-phase production	1.34	1.61	2.24	1.10	1.91	1.65	1.05	1.56	1.19	
dry deposition	−0.25	−0.16	−0.41	−0.23	−0.19	−0.48	−0.27	−0.16	−0.24	−0.44
wet deposition	−1.57	−1.80	−1.42	−1.46	−1.80	−1.33	−0.81	−1.75	−1.09	−0.82
inferred export	−0.76	−0.89	−0.80	−0.76	−0.60	−0.94	−0.97	−0.37	−0.81	−0.84
column burden	6.44	7.82	7.01	6.05	4.70	7.62	7.70	6.53	6.32	5.02

SEA DJF	CA	CB	CC	CE	CF	GA	GB	GC	GD	HA
emissions	0.06	0.08	0.05	0.08	0.06	0.10	0.14	0.00	0.00	
gas-phase production	0.38	0.42	0.08	0.38	0.22	0.32	0.29	0.30	0.20	
aqueous-phase production	0.94	0.80	1.09	0.68	1.26	0.83	0.94	1.59	1.32	
dry deposition	−0.19	−0.13	−0.19	−0.13	−0.08	−0.20	−0.20	−0.21	−0.17	
wet deposition	−0.95	−0.83	−0.75	−0.75	−1.36	−0.62	−0.93	−1.00	−1.03	
inferred export	−0.25	−0.34	−0.27	−0.26	−0.09	−0.43	−0.24	−0.68	−0.32	
column burden	4.35	4.15	3.08	3.25	1.76	3.14	3.20	6.17	3.60	
SEA JJA										
emissions	0.05	0.08	0.05	0.06	0.05	0.08	0.11	0.00	0.00	
gas-phase production	0.83	0.58	0.18	0.47	0.20	0.54	0.44	0.53	0.60	
aqeous-phase production	0.62	1.21	1.37	0.74	1.48	1.55	0.76	1.15	1.09	
dry deposition	−0.14	−0.09	−0.28	−0.08	−0.10	−0.25	−0.16	−0.09	−0.27	
wet deposition	−1.03	−1.52	−0.86	−1.16	−1.36	−1.56	−1.11	−1.57	−1.80	
inferred export	−0.33	−0.26	−0.46	−0.03	−0.27	−0.36	−0.06	−0.01	0.39	
column burden	3.06	5.16	4.51	2.47	3.26	5.25	5.27	3.34	4.90	

[1]HA does not distinguish between gas phase and aqueous phase oxidation of SO_2; Table lists total oxidation.

Table 5. *Simulated seasonal and regional budgets for sulfate; column burdens are in mg S m^{-2}; fluxes in mg S m^{-2} day^{-1}; average, standard deviation (σ) and relative contribution*

	DJF			JJA		
	average	σ	%	average	σ	%
ENA						
emissions	0.07	0.04	8	0.06	0.04	4
gas-phase production	0.13	0.05	14	0.55	0.25	37
aqueous-phase production	0.71	0.31	78	0.87	0.37	59
total production	*0.84*	*0.28*		*1.38*	*0.30*	
dry deposition	−0.12	0.06	−13	−0.17	0.09	−12
wet deposition	−0.61	0.26	−67	−1.03	0.33	−71
inferred export	−0.18	0.14	−20	−0.25	0.20	−17
column burden	2.39	0.75		4.24	1.23	
EMEP						
emissions	0.24	0.14	16	0.15	0.08	6
gas-phase production	0.12	0.05	8	0.83	0.30	33
aqueous-phase production	1.15	0.75	76	1.56	0.40	61
total production	*1.31*	*0.68*		*2.33*	*0.32*	
dry deposition	−0.18	0.12	−12	−0.29	0.12	−12
wet deposition	−0.78	0.38	−50	−1.42	0.38	−57
inferred export	−0.59	0.52	−38	−0.77	0.19	−31
column burden	3.27	1.36		6.54	1.14	
SEA						
emissions	0.07	0.04	5	0.06	0.03	4
gas-phase production	0.30	0.11	22	0.47	0.21	29
aqueous-phase production	1.02	0.29	73	1.11	0.36	67
total production	*1.31*	*0.27*		*1.58*	*0.30*	
dry deposition	−0.17	0.05	−12	−0.15	0.08	−9
wet deposition	−0.90	0.22	−65	−1.27	0.27	−77
inferred export	−0.32	0.17	−23	−0.22	0.17	−14
column burden	3.64	1.29		4.04	1.13	

Panels b and c in Figs. 5, 6 and 7 show efficiencies of dry and wet deposition of sulfate. For dry deposition, the model-to-model variability is approximately a factor of 2, except for HA which stands out with a relatively high deposition efficiency. Calculated wet deposition efficiencies vary widely between models, generally ranging from 0.1 to 0.5 day^{-1}. CF stands out in winter in each region with an efficiency of 0.8–1.2 day^{-1}. There is no consistency between models regarding the seasonality of sulfate wet deposition. The differences in parameterizations used for, for example, nucleation scavenging and below-cloud scavenging determine the sulfate amount taken up in drops to an important extent, as does the efficiency of aqueous phase SO_2 oxidation. Modeled cloud and rain (micro-)physics contribute to the model-to-model variability. However, the parameterizations applied for these processes were not examined further in our intercomparison.

Panels d show the simulated sulfate lifetimes in winter and summer. The sulfate column lifetimes also vary considerably between models. There is no general consensus about the seasonality of the sulfate lifetime. For most models the summer and winter lifetimes are of the same order, but larger-than-average seasonal differences are simulated by CE (ENA and SEA) and CF and GB (EMEP). GC stands out with a sulfate lifetime in winter for EMEP that is about twice that of the other models, related to a very small wet deposition efficiency, whereas GB simulates a relatively long lifetime for EMEP in summer, also associated with a relatively small wet deposition efficiency. Generally, an anti-correlation exists between the modeled seasonalities of sulfate wet deposition

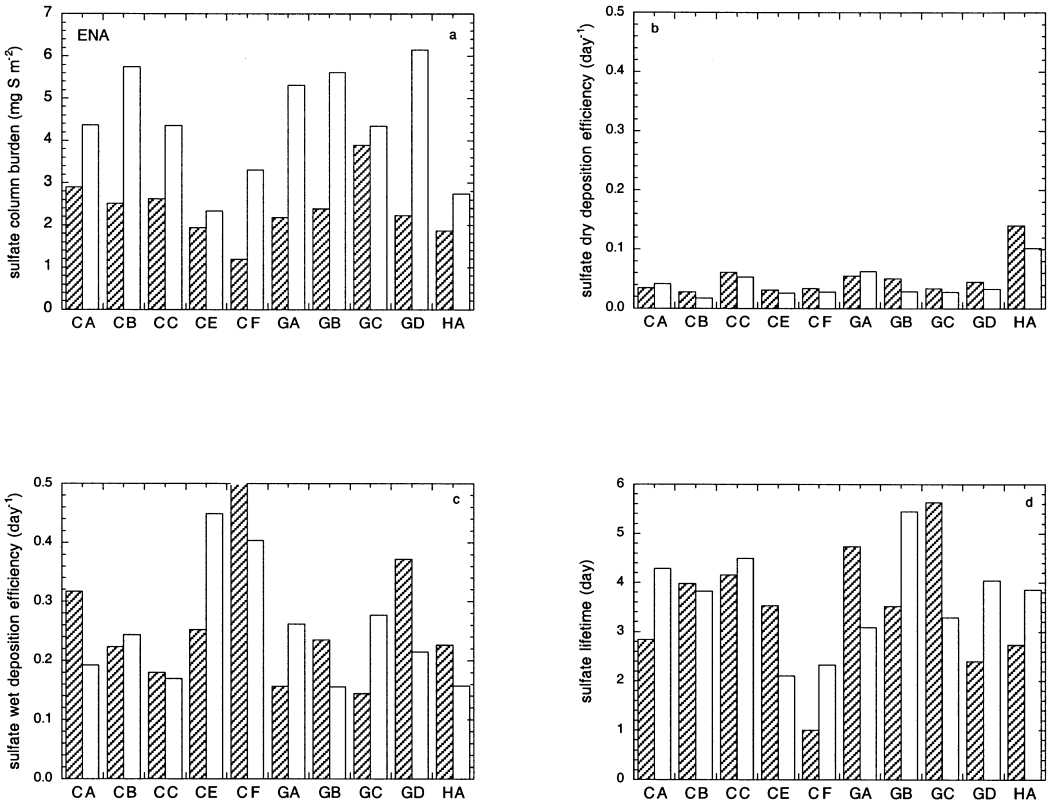

Fig. 5. Simulated sulfate budget and removal terms for the ENA region. (a) Column burden (mg S m^{-2}), (b) dry deposition efficiency (day^{-1}), (c) wet deposition efficiency (day^{-1}), and (d) lifetime (day). Seasons are DJF (shaded bars) and JJA (white bars).

and the sulfate lifetime, so that more efficient wet deposition in summer than in winter leads to smaller lifetimes in summer than in winter and vice versa. It must be noted that the definition of the SO_2 wet deposition affects the sulfate lifetime somewhat. If in-cloud produced sulfate is accounted for in the SO_2 budget, the loss is not accounted for in the sulfate lifetime, which becomes somewhat larger. In CC and GC, simulated sulfate concentrations are directly coupled to the microphysics parameterizations for large scale clouds. Larger sulfate concentrations produce more cloud droplets, which in turn reduce precipitation efficiencies. Lohmann and Feichter (1997) show that this coupling may lead to simulated sulfate lifetimes that are significantly longer. The small wet removal efficiency and long sulfate lifetime simulated by GC in EMEP in winter may be attributed to this feedback, but it is not apparent in CC.

3.3. *Partitioning between SO_2 and sulfate*

Fig. 8 shows the amount of sulfate relative to the total sulfur (SO_2 plus sulfate) column budgets for the ENA, EMEP and SEA regions. The sulfate fraction is determined by the source rates of sulfate on one hand, which are dominated by the oxidation of SO_2 in the gaseous and aqueous phase, and dry and wet deposition of sulfate on the other. All models simulate a larger sulfate fraction in summer than in winter, up to a factor of two in most models, due to more efficient oxidation of SO_2. In summer, the sulfate fraction is between 40 and 70% for all three regions. During winter the fraction is 10–35% for EMEP and 20 to 50%

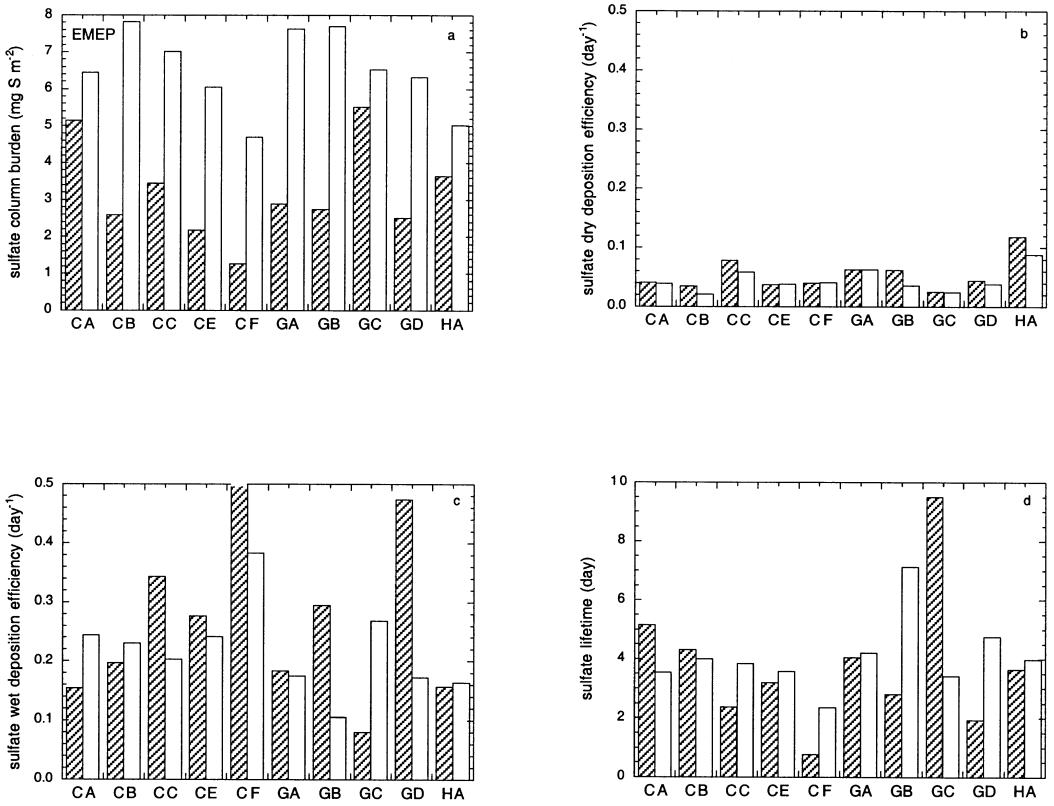

Fig. 6. As Fig. 5 but for the EMEP region.

for ENA and SEA. Differences between models are relatively larger in winter, when gas phase oxidation is relatively inefficient. For example, CA, CC and GC consistently simulate a relatively large sulfate fraction in winter. For CA and CC this is associated with relatively efficient dry deposition and aqueous phase oxidation of SO_2 (panels b and e in Figs. 2, 3 and 4) whereas for GC it is associated with a relatively inefficient sulfate wet deposition (panel c in Figs. 5, 6 and 7). CF and GD, on the other hand, simulate efficient dry deposition and aqueous phase oxidation of SO_2 as well, but also efficient wet deposition of sulfate, so that their computed sulfate fraction is somewhat smaller.

4. Vertical distribution of trace species

In this section, we briefly discuss the vertical distribution of column integrated trace species amounts, since the efficiency of most processes varies with altitude. For example, dry deposition occurs only at the surface, and aqueous phase oxidation efficiency is related to the vertical distribution of cloud occurrence. We examine the simulated vertical transport efficiencies, determined predominantly by vertical diffusion and convection, in a qualitative way based on the simulated vertical distributions of trace species.

Fig. 9 shows the partitioning below and above 2.5 km altitude for Rn, SO_2 and sulfate for the EMEP region. The Rn source and sink are the same in each model, so that the vertical distributions of Rn are indicative of the vertical transport efficiencies simulated by the models. Note that CD submitted data for Rn and Pb and not for the sulfur cycle, whereas GA submitted data for the sulfur cycle only. The simulated fraction of Rn above 2.5 km altitude is between 15–45% throughout the year. Most models simulate a larger fraction of Rn above 2.5 km altitude in summer than

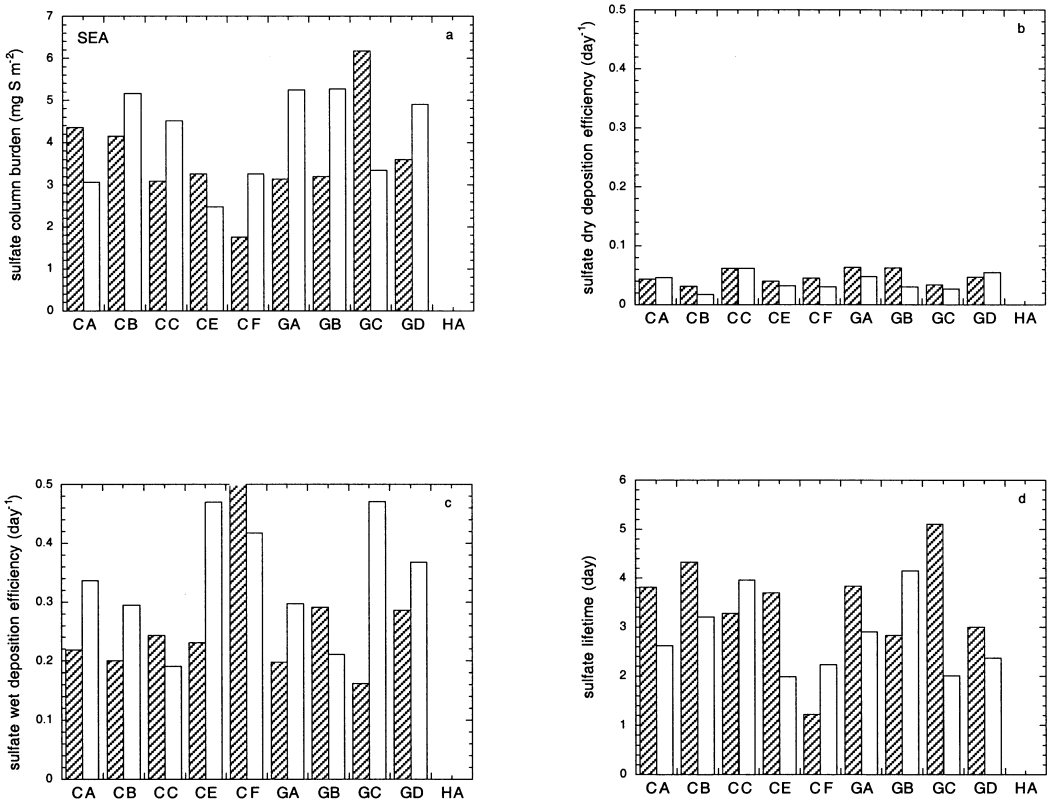

Fig. 7. As Fig. 5 but for the SEA region.

in winter, which is associated with the seasonality of convective activity. CD, CE, CF and GB simulate a relatively strong seasonality of the convective transport efficiency. In GC the upward transport is rather weak compared to the other models. A relation between the number of layers in the participating models (Table 1a) and the simulated vertical distributions of Rn is not found. Also, there is no clear distinction between models using a variable for turbulent kinetic energy and using the mixing length approach (see Table 1b). We note that the fraction of Rn above 2.5 km is larger in ENA and SEA than in EMEP, not shown here. Apparently, the fact that the efficiency of convective transports increases equatorward is modeled consistently between models.

The fraction of SO_2 present above 2.5 km is below 25% in all models. The models CA, CC, GC and GD consistently simulate that less than 10% of the SO_2 column resides above 2.5 km altitude throughout the year. For GC this may be related to relatively inefficient vertical transport as derived from Fig. 9a. For the other models it is probably associated with efficient aqueous phase oxidation and, consequently, short SO_2 lifetimes (Figs. 3, 4). HA, CB and GB simulate a relatively small, and CE and CF a large seasonal dependence of the vertical distribution.

Generally, between 40 and 60% of the column sulfate resides above 2.5 km altitude. The consistency between the models is remarkable, with a somewhat larger fraction simulated by GB and a smaller fraction by GC. Also, in most models the distribution of sulfate below and above 2.5 km does not change much with season. This suggests a compensating effect between vertical transport efficiency and the height dependence of individual processes leading to wet removal of sulfate (nucleation scavenging, impaction scavenging), although a detailed study is necessary to investigate this further. We note that simulated sulfate budgets for ENA and SEA show qualitatively similar

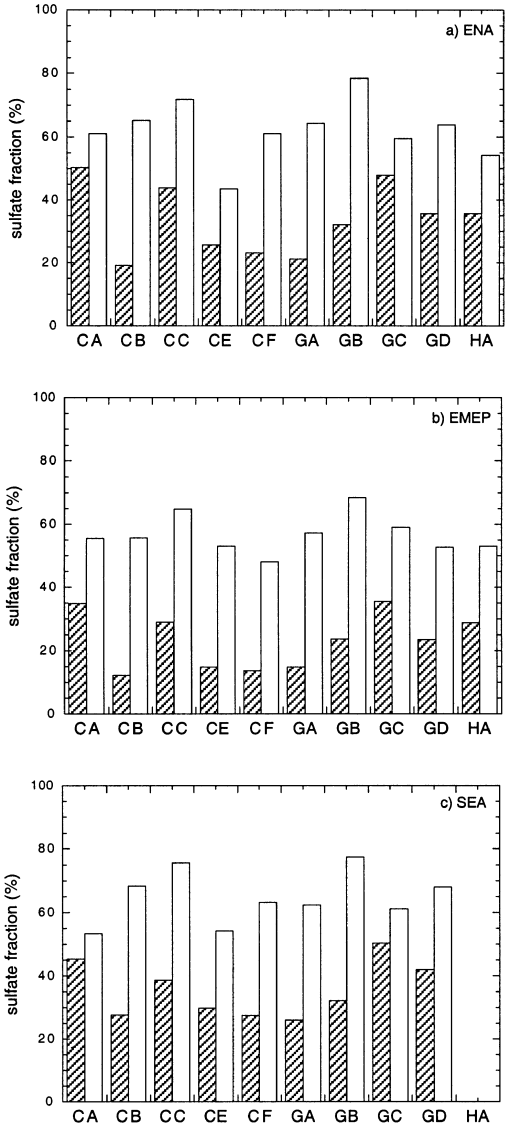

Fig. 8. Sulfur column sulfate fraction for (a) ENA, (b) EMEP, and (c) SEA, for DJF (shaded bars) and JJA (white bars).

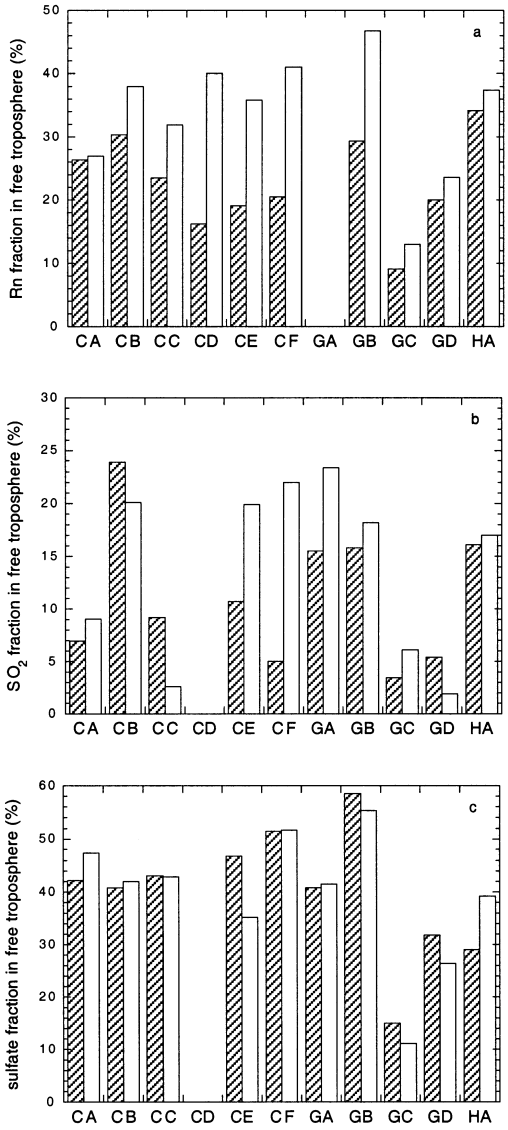

Fig. 9. Fraction residing above 2.5 km altitude of (a) Rn, (b) SO2 and (c) sulfate, for DJF (shaded bars) and JJA (white bars) for the EMEP region.

characteristics as for EMEP, although relative differences between models are larger.

5. Regional sulfur exports

As noted earlier, we inferred regional export terms by calculating the residual of the seasonal SO_2 and sulfate column sources and sinks. If a model produces a balanced budget of sources and sinks (which is the case for all participating models except GD), the inferred export term is equal to the mass fluxes of the sulfur species integrated over a season and over the region boundaries. The residual represents a net export term (or

import when the term is positive). It is, in turn, a residual of separate import and export budgets, the first acting as an additional source and the second as an additional sink. The residual calculation does not provide values for the separate import and export budgets, so that a first order export efficiency cannot be calculated.

In this section, we do not separate SO_2 and sulfate exports. If we assume SO_2 to be removed only by oxidation, it is evident that the total amount of exported SO_2 will be larger, and that of sulfate smaller, if the regional boundaries are located closer to the source. The opposite is true if the distance between boundaries and source is larger. Since the regional boundaries are chosen quite arbitrarily, the distribution of sulfur export between SO_2 and sulfate is irrelevant. Therefore we consider the export of total sulfur (SO_x), so that differences between models in the SO_2 oxidation efficiency are compensated to some extent while differences in deposition rates, which determine the lifetime of sulfur in the atmosphere, are accentuated.

Fig. 10 shows regional column burdens and the inferred export budget terms for SO_x for all models except GD. SO_2 emissions are about the same in the models, so that the differences between simulated SO_x columns are associated with the simulated SO_x removal efficiencies, i.e., the deposition rates for SO_2 and sulfate. Consequently, similar differences apply to the sulfur export terms. Nevertheless, the export of SO_x from the EMEP region in winter is simulated quite consistently between models, except for CF who computes smaller terms. In this case the simulation of the sulfur budget is quite straightforward. In winter, most sulfur is in the form of SO_2 and present in the lower troposphere (Figs. 8, 9). SO_2 dry deposition, which is an important sink term in winter, is simulated quite consistently between models, as seen in Fig. 3b, and as a consequence the range in calculated SO_x exports is relatively small. However, the relative differences between models are larger in summer when processes with larger relative model uncertainties become important, such as cloud chemistry and convective transports. For the same reasons, relative differences are somewhat larger in ENA and SEA regions than in EMEP. Differences between models for the simulated export of SO_x range from a factor of two up to an order of magnitude depending on region and season. There is no apparent consensus about the seasonality of export budgets, apart from EMEP where it may be dominated by the seasonality of sulfur emissions. In CF, export in winter is relatively small due to efficient sulfate wet deposition.

6. Conclusions and discussion

We investigated and compared budgets for SO_2 and sulfate for three regions in the Northern Hemisphere, simulated by one hemispheric and nine global sulfur cycle models, in order to identify processes in the sulfur cycle that are subject to relatively large model-to-model variability. The emissions, which are prescribed, are consistent between models, although small differences occur which are related to definitions of the domain. The trace species distribution between the lower and the free troposphere, mainly associated with simulated vertical transports, varies strongly between models, especially in summer. The associated seasonality suggests that the simulation of convective transports plays an important rôle in this. We found no clear relation between the vertical distribution of tracers and the vertical model resolution. Models with relatively efficient vertical transports throughout the year are GA, GB, and CB, while they appear to be less efficient in GC. We note that the simulated distributions of trace species between the lower and free troposphere may change away from source regions, as illustrated by an analysis of simulated Rn profiles over the North Atlantic region by Lohmann et al. (2001).

The efficiency of dry deposition of SO_2 and sulfate varies by about a factor of 3 between models, probably due to the parameterization of the leaf area index (LAI) and soil humidity. Wet deposition is of relatively small importance in the SO_2 budget, although models are not consistent in their budgeting of this process. On the other hand, wet deposition is a dominant factor in the sulfate budget. Its efficiency in removing sulfate from the atmosphere is about $5\times$ that of dry deposition. In most models, 40–60% of the sulfate resides above 2.5 km altitude in the three regions; this fraction varies relatively little with season.

For the SO_2 dry deposition efficiency, there appears to be a distinction within the group CTMs

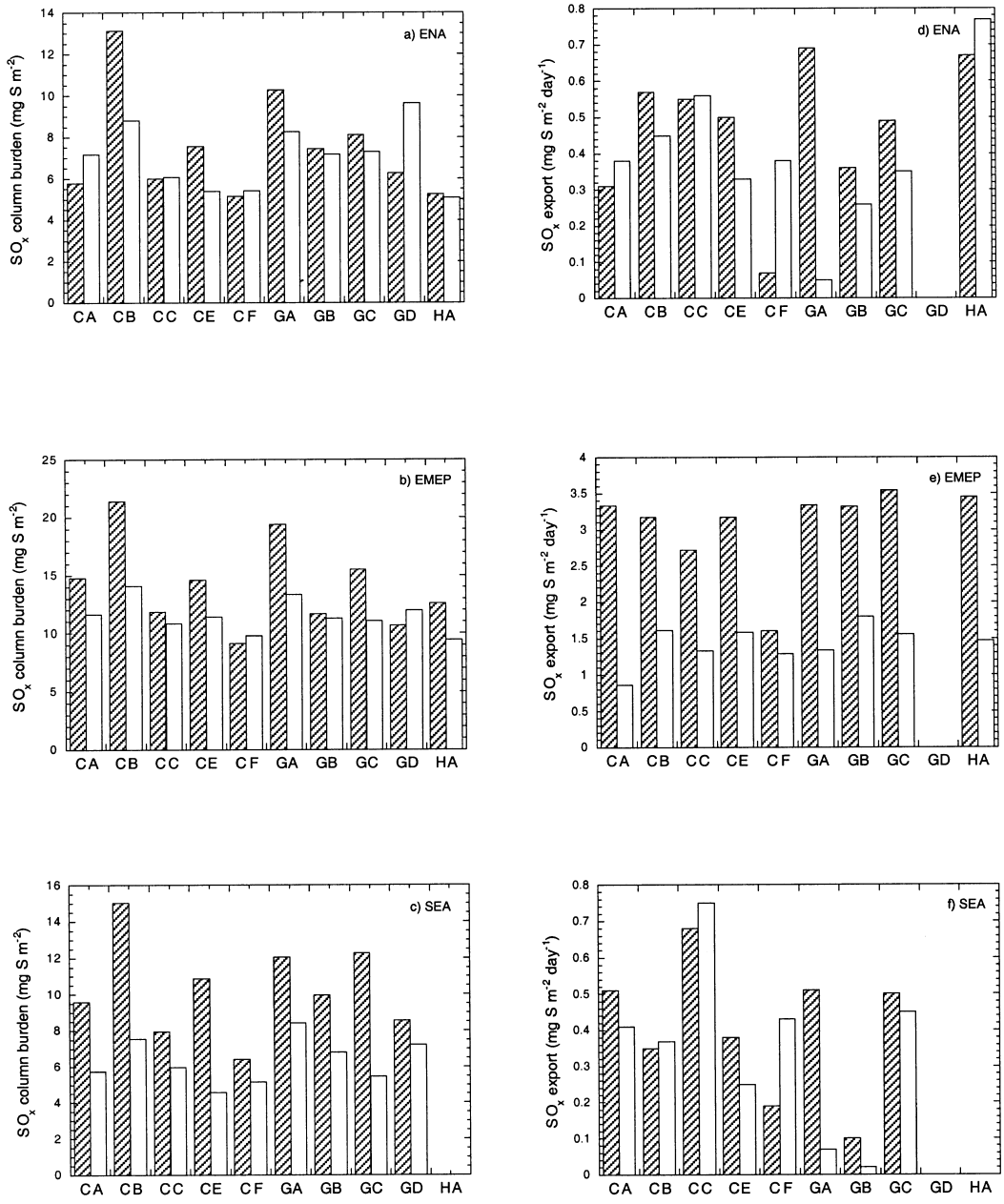

Fig. 10. Simulated column SO_x burden (mg S m^{-2}) for (a) ENA, (b) EMEP and (c) SEA; inferred export of SO_x (mg S m^{-2} day^{-1}) out of (d) ENA, (e) EMEP and (f) SEA, for DJF (shaded bars) and JJA (white bars).

between those with a relatively high (CA, CC, CF) and a relatively low vertical resolution (CB, CE). A higher vertical resolution apparently attenuates mixing between the boundary layer and the free troposphere, thereby enhancing the impact of dry deposition of sulfur species. A relation is also found between the vertical resolution and the aqueous phase oxidation efficiency, although more

detailed studies are needed to explain this. In general, the effect of resolution, both horizontal and vertical, appears to be minor compared to other differences when all models are considered.

While there are general similarities in model regional sulfate budgets, we find significant differences when the collection of models is considered. Particularly significant from a sulfate budget standpoint is the fact that in any given region and season, there is a considerable range in the simulated aqueous-phase sulfate production rates, wet deposition efficiencies, and upward transport efficiencies. Consequently, the simulated lifetimes of SO_2 and sulfate differ within a large range. For example, in ENA these are between 1–5 days for SO_2 in winter and 2–7 days for sulfate in summer. Simulated wet deposition rates for sulfate range over a factor of 4, whereas one model stands out even more with a very high wet deposition efficiency. We note that a clear relation between the model resolution and the sulfate formation and removal efficiencies is not found.

When the standard deviation of the modeled budgets is used as a measure (Tables 3, 5), cloud-related processes in the sulfur cycle display the largest model-to-model variabilities. This suggests that the dominant cause of differences between models in the sulfur cycle simulation is the representation of (sub-grid) cloud characteristics. We remark that Barrie et al. (2001) find a clear difference between GCMs and CTMs for the simulation of Rn/Pb where the chemical transformation has a constant rate, but that the difference is less evident for the sulfur cycle where aqueous phase processes dominate transformation. Therefore, we suggest that a first effort in improving the representativity of global sulfur cycle models should at least address the validation of spatial and temporal distributions of simulated cloud fields, especially those associated with microphysical processes that are crucial for the chemical transformation and the removal of sulfur species, i.e., nucleation on aerosols and precipitation formation. We also recommend that a comparison with observed wet deposition fluxes is carried out to assess the representativity of computed wet deposition fluxes.

The results indicate that the simulated aqueous phase SO_2 oxidation efficiency in winter depends on how models represent oxidant chemistry ("imported" versus "full" or "prognostic", see Table 1). The models with full or prognostic models simulate less efficient SO_2 oxidation as a result of oxidant limitation in polluted regions. Differences are also manifested otherwise: Lohmann et al. (2001) found a significant difference between models using full and imported oxidant chemistry when they compared modeled and observed SO_2 and sulfate vertical profiles for the relatively clean North Atlantic region (NARE).

The models do not agree about the magnitude of sulfur exports from polluted regions to cleaner areas, and show differences up to an order of magnitude in summer (although variabilities in the separate SO_2 and sulfate budget terms are compensated to some extent when SO_x is considered). Although we have not analyzed the simulated budgets over remote regions, it may be expected that sulfur column budgets and the vertical distributions in remote areas show a large model-to-model variability as well. This will affect estimates of the direct and indirect climate forcing by sulfate aerosol, and the related uncertainty is probably comparable to the uncertainties presented in this study.

7. Acknowledgements

The first author wishes to thank the Netherlands Organization for Scientific Research for funding (NOP-II project 951258).

REFERENCES

Albrecht, B. A. 1989. Aerosols, cloud microphysics, and fractional cloudiness. *Science* **245**, 1227–1230.

Benkovitz, C. M., Scholtz, M. T., Pacyna, J., Tarrasón, L., Dignon, J., Voldner, E. C., Spiro, P. A., Logan, J. A. and Graedel, T. E. 1996. Global gridded inventories of anthropogenic emissions of sulfur and nitrogen. *J. Geophys. Res.* **101**, 29,239–29,253.

Benkovitz, C. M. and Schwartz S. E. 1997. Evaluation of modeled sulfate and SO_2 over North America and Europe for four seasonal months in 1986–1987. *J. Geophys. Res.* **102**, 25,305–25,338.

Boucher, O. and Lohmann, U. 1995. The sulfate-CCN-cloud albedo effect: a sensitivity study with two general circulation models. *Tellus* **47B**, 281–300.

Charlson, R. J., Schwartz, S. E., Hales, J. M., Cess, R. D., Coakley, J. A., Hansen, J. E. and Hofmann, D. J. 1992.

Climate forcing by anthropogenic aerosols. *Science* **255**, 423–430.

Chin, M., Jacob, D. J., Gardner, G. M., Foreman-Fowler, M., Spiro, P. A. and Savoie, D. L. 1996. A global three-dimensional model of tropospheric sulfate. *J. Geophys. Res.* **101**, 18,667–18,690.

Chin, M., Rood, R., Lin, S. J., Jacob, D., Müller, J. F. and Thompson, A. 2000. Atmospheric sulfur cycle simulated in the global model GOCART. *J. Geophys. Res.* **105**, 24,689–24,712.

Christensen, J. H. 1997. The Danish Eulerian hemispheric model — a three-dimensional air pollution model used for the Arctic. *Atmos. Environ.* **31**, 4169–4191.

Crutzen, P. J. and Zimmermann, P. H. 1991. The changing photochemistry of the troposphere. *Tellus* **43AB**, 136–151.

Dentener, F., Feichter, J. and Jeuken, A. 1999. Simulation of ^{222}Rn using on-line and off-line global models at different horizontal resolutions: A detailed comparison with measurements. *Tellus* **51B**, 573–602.

Feichter, J., Kjellström, E., Rodhe, H., Dentener, F., Lelieveld, J. and Roelofs, G. J. 1996. Simulation of the tropospheric sulfur cycle in a global climate model. *Atmos. Environ.* **30**, 1693–1707.

Ghan, S. J., Laulainen, N. S., Easter, R. C., Wagener, R., Nemesure, S., Chapman, E. G., Zhang, Y. and Leung, L. R. 2001. Evaluation of aerosol direct radiative forcing in MIRAGE. *J. Geophys. Res.*, in press.

Ganzeveld, L., Lelieveld, J. and Roelofs, G. J. 1998. A dry deposition parameterization for sulfur oxides in a chemistry and general circulation model. *J. Geophys. Res.* **103**, 5679–5694.

Garret, T. J. and Hobbs P. V. 1995. Long range transport of continental aerosol and their effect on cloud structures. *J. Atmos. Sci.* **52**, 2977–2984.

Jones, A., Roberts, D. L. and Slingo, A. 1994. A climate model study of the indirect radiative forcing by anthropogenic sulfate aerosols. *Nature* **370**, 450–453.

Kasibhatla, P., Chameides, W. L. and John, J. St. 1997. A three dimensional global model investigation of seasonal variations in the atmospheric burden of anthropogenic sulfate aerosols. *J. Geophys. Res.* **102**, 3737–3760.

Kiehl, J. T. and Briegleb, B. P. 1993. The relative roles of sulfate aerosols and greenhouse gases in climate forcing. *Science* **260**, 311–314.

Koch, D. M., Jacob, D. J., Rind, D. Chin, M. and Tegen, I. 1999. Tropospheric sulfur simulation and sulfate direct radiative forcing in the Goddard Institute for Space Studies general circulation model. *J. Geophys. Res.* **104**, 23,799–23,822.

Langner, J. and Rodhe, H. 1991. A global three-dimensional model of the global sulfur cycle. *J. Atmos. Chem.* **13**, 225–236.

Law, K. S., Plantevin, P. H., Shallcross, D. E., Rogers, H., Grouhel, C., Thouret, V., Marenco, A. and Pyle, J. A. 1998. Evaluation of modeled O_3 using MOZAIC data. *J. Geophys. Res.* **103**, 25,721–25,740.

Lohmann, U. and Feichter, J. 1997. Impact of sulfate aerosols on albedo and lifetime of clouds: a sensitivity study with the ECHAM4 GCM. *J. Geophys. Res.* **102**, 13685–13700.

Lohmann, U., Von Salzen, K., McFarlane, N., Leighton, H. G. and Feichter, J. 1999. The tropospheric sulfur cycle in the Canadian general circulation model. *J. Geophys. Res.* **104**, 26,833–26,858.

Mahowald, N. M., Rasch, P. J. and Prinn, R. G. 1995. Cumulus parameterization in chemical transport models. *J. Geophys. Res.* **100**, 26,173–26,189.

Penner, J. E., Bergmann, D., Walton, J. J., Kinnison, D., Prather, M. J., Rotman, D., Price, C., Pickering, K. E. and Baughcum, S. L. 1998. An evaluation of upper tropospheric NO_x with two models. *J. Geophys. Res.* **103**, 22,097–22,113.

Pham, M., Müller, J.-F., Brasseur, G. P., Granier, C. and Mégie, G. 1995. A three-dimensional study of the tropospheric sulfur cycle. *J. Geophys. Res.* **100**, 26,061–26,092.

Radke, L. F., Coagley, J. A. jr, and King M. D. 1989. Direct and remote sensing observations of the effects of ships on clouds. *Science* **246**, 1146–1149.

Rasch P. J., Mahowald, N. M. and Eaton, B. E. 1997. Representations of transport, convection, and the hydrologic cycle in chemical transport models: implications for the modeling of short-lived and soluble species. *J. Geophys. Res.* **102**, 28,127–28,138.

Roelofs, G. J., Ganzeveld, L. G. and Lelieveld, J. 1998. Simulation of global sulfate distribution and the influence on effective cloud drop radii with a coupled photochemistry–sulfur cycle model. *Tellus* **50B**, 224–242.

Schimel, D. et al., 1996. Radiative forcing of climate change. In: *Climate Change 1995*, edited by J. T. Houghton, L. G. Meira Filho, B. A. Callander, N. Harris, A. Kattenberg and K. Maskell, Cambridge University Press, Cambridge, pp. 65–130.

Spiro, P. A., Jacob, D. J. and Logan, J. A. 1992. Global inventory of sulfur emissions with 1°x1° resolution. *J. Geophys. Res.* **97**, 6023–6036.

Twomey, S. 1974. Pollution and the planetary albedo. *Atmos. Environ.* **8**, 1251–1256.